Intramolecular Hydrogen Bonding in Bisphenol Developing Agents for Photothermographic Application

Hiromi Akahori, Kiyokazu Morita, Ayumu Nishijima, and Tsuyoshi Mitsuhashi
R&D Center, Konica Minolta Medical & Graphic, Inc., Hino, Tokyo, JAPAN

Kei Ohkubo and Shunichi Fukuzumi
Department of Material and Life Science, Graduate School of Engineering, Osaka University, SORST, Japan Science and Technology Agency (JST)
Suita, Osaka, JAPAN

The effects of intramolecular hydrogen bonding on the electron transfer properties of a series of bisphenol derivatives, as compared with those of monophenol derivatives in which a hydroxy group of the bisphenols is replaced with a methoxy group, have been investigated in relation to their utility as photothermographic developers. The oxidation of bisphenol derivatives with one-electron oxidants occurs to give the radical cation, followed by deprotonation, to produce the phenoxyl radical. Both the radical cations and phenoxyl radicals have been detected by laser flash photolysis measurements. Rates of hydrogen transfer reactions from a series of bisphenol derivatives to cumylperoxyl radicals have also been determined by monitoring the decay of the ESR signal of cumylperoxyl radical produced by photoirradiation of an oxygen saturated propionitrile solution of cumene and di-*t*-butylperoxide in the presence of the bisphenol derivatives. Intramolecular hydrogen bonding plays an important role in determining the overall oxidation reactivity in the two-electron oxidation process of bisphenol derivatives by decreasing the one-electron oxidation potentials and also by facilitating the deprotonation step from the bisphenol radical cation to produce a phenoxyl radical.

Introduction

Social concerns over the protection of the environment have grown in recent years. At the same time, the digitization and networking of medical imaging information have made remarkable advances. Such social concerns together with the technological advances have led to the design and development of dry processing imaging systems using photothermographic materials. The image formation mechanism of the photothermographic system consists of four major steps.[1] In the first step, the photothermographic film is exposed to light, producing latent images on the surface of silver halide particles. In the second step, the photothermographic film is heated to approximately 393 K. In the third step, in response to this heating, silver carboxylates may react with phthalic acid to produce silver phthalate, which then reacts with phthalazine to produce a silver phthalazine complex. Subsequently, the silver ions are transported to the latent images as silver/toner complexes. In the final step, these silver ions are thermally reduced by the developing reagent to produce developed metallic silver. One objective in designing a dry processing imaging system is to optimize the photothermographic properties of the system. In order to optimize these properties, it is essential to control the reactivity of the developer reagent. Bisphenol derivatives have recently merited particular interest as efficient developers in photothermographic systems,[1,2] and they are also known to perform well as antioxidants and stabilizers.[3,4] However, little is know about the relationships between the chemical structures of bisphenol derivatives and their electron transfer and developing properties. Intramolecular hydrogen bonding is recognized to play an important role in the reactivity of the phenolic function.[4] The hydrogen bonding in bisphenol derivatives can stabilize not only the phenol form but also the phenoxyl radical form.[5] However, up to now, there has been no systematic study with regard to the effects of intramolecular hydrogen bonding on the electron transfer properties of bisphenol derivatives.

We therefore decided to investigate the effects of the intramolecular hydrogen bonding on the electron transfer properties of bisphenol derivatives in relation to their photothermographic reactivity in silver salt photothermographic systems. We examined the electron transfer properties of four bisphenol derivatives with different substituents (R_1 = methyl, ethyl, n-propyl, and t-butyl) neighboring the hydroxy groups in comparison with those of four monophenol derivatives in which one of the hydroxy groups was replaced with a methoxy group (Fig. 1).

R₁ = Me, Et, *n*-Pr, *t*-Bu
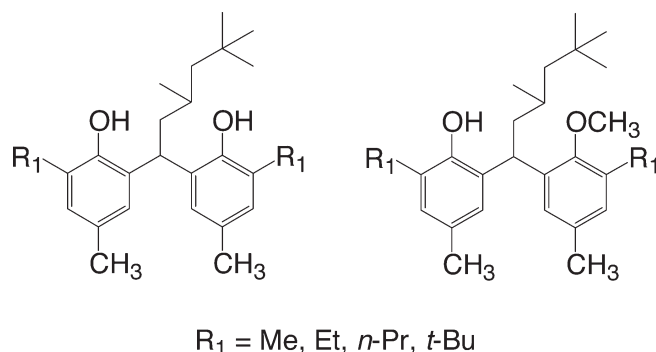
Figure 1. Chemical structures of bisphenol derivatives and monophenol derivatives.

A proposed mechanism for the two-electron oxidation of this compound is shown in Scheme 1.[1] In an earlier study,[2] the differential pulse voltammograms of all eight compounds were measured to determine their one-electron oxidation potentials (E^0_{ox}). The investigation of chemical oxidation using one-electron oxidants such as $Fe(bpy)_3^{3+}$ (bpy = 2,2'-bipyridine) was also performed to determine their oxidation rate constants. In addition, electron spin resonance (ESR) was used to detect the intermediate radical species, i.e., the phenoxyl radicals, so that the overall reactivity of the two-electron oxidation process can be evaluated. The hyperfine structure of the phenoxyl radicals was well resolved, and the hyperfine coupling constants were determined by comparing the ESR spectra with the computer simulation spectra. The ESR analysis leads to conclusion such that the phenoxyl radical forms an intramolecular hydrogen bond with the proton of OH group of each bisphenol derivative. The intramolecular hydrogen bond has a decisive impact on the reactivity of bisphenol derivatives during the oxidation process.

Scheme 1
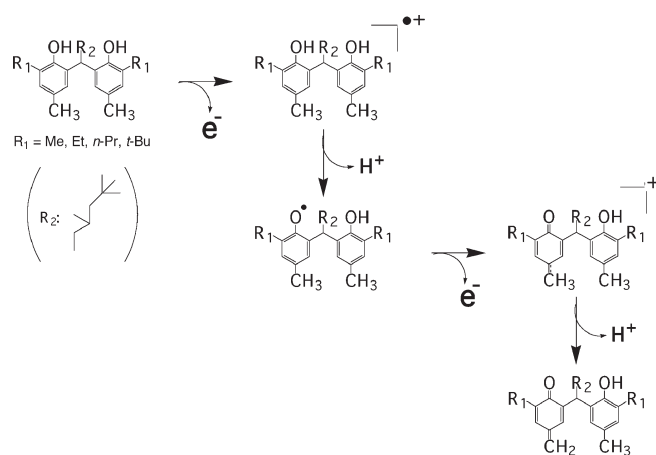
This article is focused on detection of the oxidation intermediate, i.e., the radical cation species, and determination of the rate constants of the deprotonation in order to clarify the effects of the intramolecular hydrogen bonding on the structure of the oxidation intermediates and the effects of the R₁ substituents on

the electron transfer properties of the bisphenol derivatives, respectively. The rate constants of the hydrogen transfer reactions of bisphenol derivatives to produce the phenoxyl radicals are also determined to reveal the relationship between the redox properties and the photothermographic developing properties of bisphenol derivatives.

Experimental
Materials
1-Bis(2-hydroxy-3,5-dimethylphenyl)-3,5,5-trimethylhexane was obtained commercially and purified by the standard method.[6] The other bisphenol derivatives were prepared according to the literature[7] and purified by the standard methods.[6] The monophenol derivatives were prepared through the methylation of corresponding bisphenol derivatives with sodium hydride and iodomethane by way of Williamson synthesis and purified by the standard methods.[6] We prepared 10-methylacridinium iodide by the reaction of acridine with methyl iodide in acetone, and it was converted to the perchlorate salt ($AcrH^+ClO_4^-$) by addition of magnesium perchlorate to the iodide salt. $AcrH^+ClO_4^-$ was purified by recrystallization from methanol.[8,9] Di-*t*-butylperoxide was purchased from Nacalai Tesque, Inc. and purified by chromatography through alumina which removes a trace of the hydroperoxide.[6] Cumene was purchased from Wako Pure Chemical Industries, Ltd. and was used as received. Acetonitrile (MeCN; spectral grade) used as solvent was purchased from Nacalai Tesque, Inc. and was used as received. Propionitrile (EtCN) used as solvent was purified and dried by the standard method.[6]

Fluorescence Quenching
Quenching of the fluorescence of $AcrH^+$ by electron donor (bisphenol or monophenol derivatives) was monitored on a Shimadzu RF-5300PC fluorescence spectrophotometer (Shimadzu Corp., Japan). The excitation wavelength was 358 nm for $AcrH^+$. The monitoring wavelengths were those corresponding to the maxima of the respective emission bands, 488 nm when the excitation wavelength was 358 nm.[10] The solutions were deoxygenated by argon purging for ca. 10 min prior to the measurements. Relative emission intensities were measured for MeCN solution containing $AcrH^+$ (2.8×10^{-5} M) with electron donors at various concentrations ($3.0 \times 10^{-4} - 1.6 \times 10^{-3}$ M). There was no change in the shape but there was a change in the intensity of the fluorescence spectrum on addition of an electron donor. The Stern–Volmer relationship (Eq. (1)),

$$I_0/I = 1 + K_{SV}[D] \tag{1}$$

was obtained for the ratio of the emission intensities in the absence and presence of quenchers (I_0/I) and the concentrations of electron donors (bisphenol or monophenol derivatives) ([D]). The fluorescence lifetime (τ) of $AcrH^+$ is 37 ns in deaerated MeCN at 298 K.[10] The quenching rate constants, k_{et} ($= K_{SV}\tau^{-1}$), were determined from the Stern–Volmer constants K_{SV} and the emission lifetimes τ.

Laser Flash Photolysis
The measurement of transient absorption spectra in the photochemical reaction of bisphenol derivatives with 10-methylacridinium cation ($AcrH^+$) was performed according to the following procedure. An MeCN solution containing a bisphenol derivative (6.0×10^{-3} M) and $AcrH^+$ (2.8×10^{-5} M) was deoxygenated by argon purging for ca. 10 minutes prior to the measurement. The

R$_1$	k_{et}, M^{-1} s^{-1}	
	bisphenol	monophenol
Me	1.8×10^{10}	1.6×10^{10}
Et	1.6×10^{10}	1.5×10^{10}
n-Pr	1.6×10^{10}	1.5×10^{10}
t-Bu	1.6×10^{10}	1.5×10^{10}

deaerated MeCN solution was excited by a Nd:YAG laser (Spectra-Physics, Inc., USA, Quanta-Ray GCR-130, 6 ns fwhm,) at 355 nm with a power of 30 mJ per pulse as an excitation source, with a continuous Xe-lamp (150 W) and an InGaAs-PIN photodiode (Hamamatsu 2949) as a probe light and detector, respectively. The output from the InGaAs-PIN photodiode was recorded with a digitizing oscilloscope (HP/Agilent Technologies, Inc., USA, 5451B, 300 MHz). The transient spectra were recorded using fresh deaerated solutions for each laser excitation. All experiments were performed at 298 K.

Kinetic Measurements
Kinetic measurements for the hydrogen transfer reactions of a series of bisphenol derivatives with cumylperoxyl radicals were performed on a JEOL X-band spectrometer (JEOL Ltd., Japan, JES-ME-LX) at 193 K. Typically, photoirradiation of an oxygen saturated EtCN solution containing di-t-butylperoxide (1.0 M) and cumene (1.0 M) with a 1000 W Mercury lamp resulted in formation of cumylperoxyl radical ($g = 2.0156$),[11] which could be detected at low temperatures. The g values were calibrated using an Mn^{2+} marker. When the light is cut off, the decay of the ESR intensity was recorded with time. The decay rate was accelerated by the presence of a bisphenol derivative, e.g., 1.0×10^{-4} M. Rates of hydrogen transfer from bisphenol derivative to cumylperoxyl radical were monitored by measuring the decay of the ESR signal of cumylperoxyl radical in the presence of various concentrations of bisphenol derivative in EtCN at 193 K. Pseudo-first order rate constants were determined by a least-squares curve fit using a microcomputer. The first order plots of $\ln\{(I - I_\infty)/(I_0 - I_\infty)\}$ versus time (I, I_∞, and I_0 denotes the ESR signal intensity at the reaction time t, the initial and the final ESR intensity, respectively) were linear for three or more half-lives with correlation coefficient, $\rho > 0.99$.

Theoretical Calculations
Density-functional theory (DFT) calculations were performed on a Compaq DS20E computer. Geometry optimizations were carried out using the Becke3LYP and 6-31G** basis set[12,13] with the restricted Hartree Fock (RHF) formalism for bisphenols and with unrestricted Hartree Fock (UHF) for their radical cations and phenoxyl radicals as implemented in the Gaussian 98 program. The ionization and deprotonation energies were determined from the energy differences between the neutral and the radical cation species and those between the parent and the phenoxyl radical species, respectively.

Evaluation of Photographic Properties (Sensitometry)
The evaluation of photographic properties was performed following standard procedure: the film samples comprising organic silver salts, silver halide grains, and other reagents were prepared according to the literature.[14] The film samples were uniformly exposed with an 810 nm laser diode and developed at a representative thermal development temperature of 399 K. Both exposure and development were performed on a Konica DRYPRO™ MODEL 722 dry laser imager.

Results and Discussion
Photoinduced Electron Transfer Oxidation of a Series of Bisphenol Derivatives and Monophenol Derivatives
Irradiation of the absorption band of 10-methyl-acridinium ion (AcrH$^+$) results in fluorescence at $\lambda = 488$ nm in deaerated MeCN.[10] The fluorescence of the singlet excited state of AcrH$^+$ (^{1}AcrH^{+*}) is quenched efficiently by a series of bisphenol derivatives in MeCN. The quenching rate constants k_{et} are determined from the slope of the Stern-Volmer plot and lifetime of the ^{1}AcrH^{+*} (37 ns).[10] The k_{et} values, summarized in Table I, close to the diffusion rate constant in MeCN (2.0×10^{10} M^{-1} s^{-1}), since the photoinduced electron transfers from bisphenol and monophenol derivatives ($E^0_{ox} = 1.1 - 1.3$ V vs SCE)[2] to ^{1}AcrH^{+*} ($E^0_{red} = 2.32$ V vs SCE)[10] are highly exergonic.[15]

Detection of the Oxidation Intermediates of a Series of Bisphenol Derivatives and Monophenol Derivatives
The oxidation intermediates of a series of bisphenol derivatives, i.e., the radical cation species in Scheme 1, were produced by photoinduced electron transfer from bisphenol derivatives to ^{1}AcrH^{+*} at room temperature (Scheme 2). The photoexcitation of the absorption band of AcrH$^+$ in a deaerated MeCN solution containing a bisphenol derivative with a laser pulse (355 nm from a Nd:YAG laser) results in the photoinduced electron transfer from the bisphenol derivative to ^{1}AcrH^{+*}. The formation of the radical cation of a bisphenol derivative is seen as the rise in the transient absorption band at 430 nm as shown in Fig. 2.[16] Subsequently, there was an increase in absorbance due to the phenoxyl radical of the bisphenol derivative, accompanied by a concomitant decrease in absorbance due to the radical cation.[16]
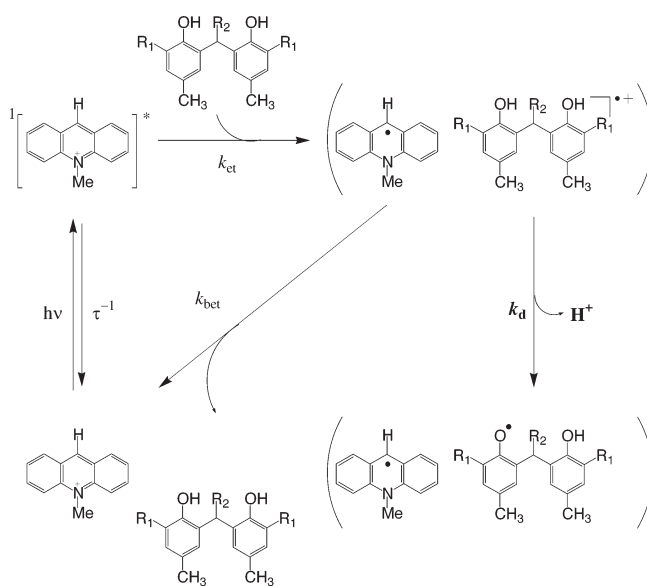
Scheme 2
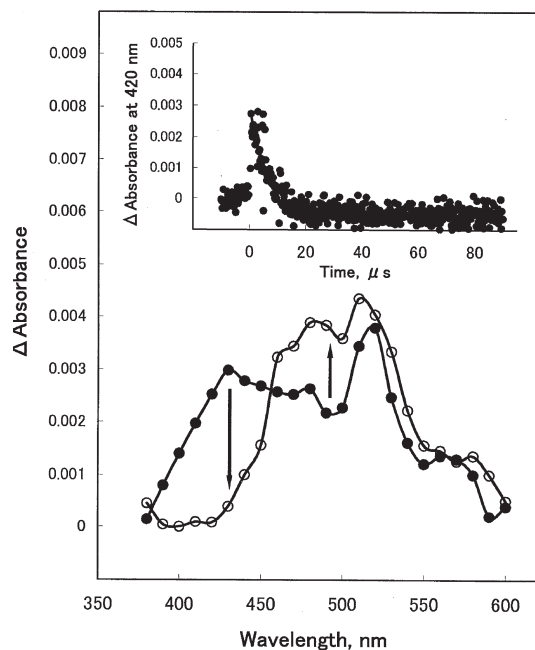
Figure 2. Transient absorption spectra measured at 2 μs (●) and 40 μs (○) after laser excitation (355 nm, 30 mJ) of AcrH⁺ (2.8 × 10⁻⁵ M) in deaerated MeCN containing a bisphenol derivative (R_1 = Me, 6.0 mM) at 298 K. Inset shows decay time profile at 420 nm.
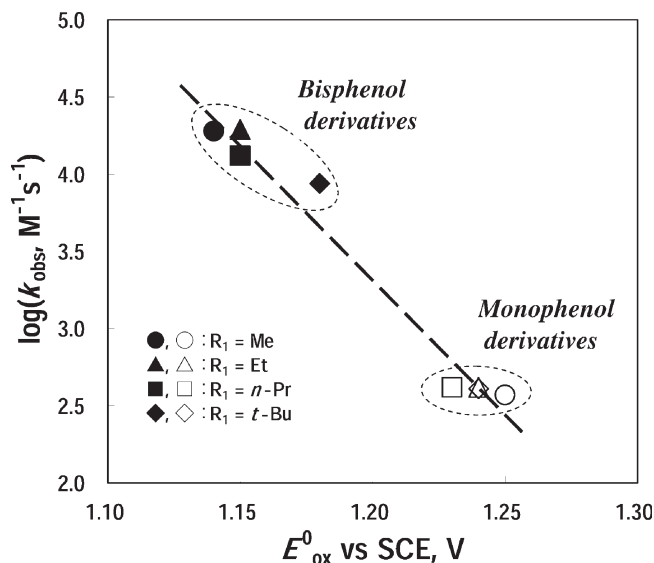
Figure 3. Plots of log k_{obs} versus E^0_{ox}; the correlation between logarithm of the observed second order rate constants for the two-electron oxidation of the bisphenol and monophenol derivatives and the one-electron oxidation potential in MeCN.

TABLE II. Rate Constants of Deprotonation from Radical Cations (k_d), Overall Rate Constants of Two-Electron Oxidation (k_{obs}), and One-Electron Oxidation Potentials (E^0_{ox}) of Bisphenol and Monophenol Derivatives

	R_1	k_d,[a] s^{-1}	k_d,[b] s^{-1}	k_{obs},[c] $M^{-1}s^{-1}$	E^0_{ox}, vs SCE, V
bisphenol	Me	1.5 x 10⁵	2.1 x 10⁵	1.9 x 10⁴	1.14
	Et	1.2 x 10⁵	3.2 x 10⁵	2.0 x 10⁴	1.15
	n-Pr	1.1 x 10⁵	2.2 x 10⁵	1.3 x 10⁴	1.15
	t-Bu	2.8 x 10⁵	4.6 x 10⁵	8.7 x 10³	1.18
monophenol	Me	1.5 x 10⁵	3.2 x 10⁵	3.7 x 10²	1.25
	Et	1.4 x 10⁵	2.2 x 10⁵	4.1 x 10²	1.24
	n-Pr	1.2 x 10⁵	1.6 x 10⁵	4.2 x 10²	1.23
	t-Bu	1.7 x 10⁵	2.3 x 10⁵	4.2 x 10²	1.24

[a] Determined from the first order decay of the radical cations.
[b] Drew from the k_{obs} and the E^0_{ox} values using Eq. (4): log k_{obs} = log $2k_d$ − (F/2.3RT)(E^0_{ox} − E^0_{red}).
[c] Determined from the electron transfer rate constant using Fe(bpy)₃³⁺.

The decay of the transient absorption band due to the radical cation obeyed first order kinetics (inset, Fig. 2). From the first order decay rate constants are determined the rate constants of deprotonation of bisphenol radical cations. The deprotonation rate constants of the radical cations of bisphenol and monophenol derivatives thus determined are virtually the same as shown in Table II.

We have recently demonstrated that there is a clear correlation between a decrease in the logarithmic values of the observed second order rate constants of the two-electron oxidation of those derivatives (log k_{obs}) and an increase in their one-electron oxidation potentials (E^0_{ox}) (Fig. 3).[2]

If the deprotonation of the radical cations of the bisphenol and monophenol derivatives (k_d) is the rate-determining step for the two-electron oxidation process, then the overall rate constant of two-electron oxidation (k_{obs}) can be expressed by Eq. (2),

Scheme 3

Akahori, et al.
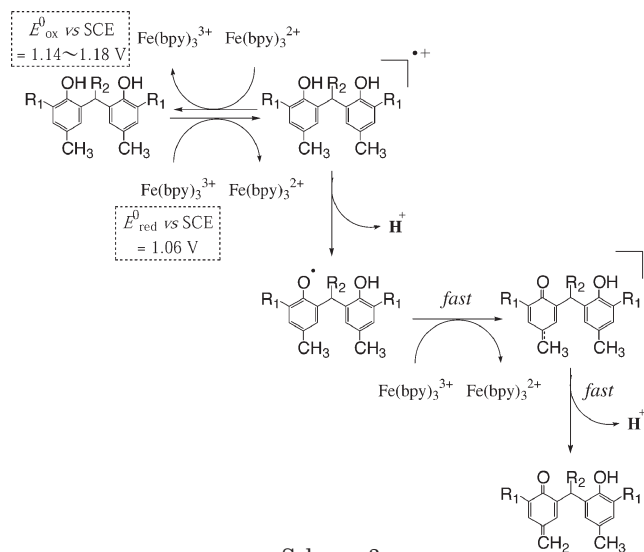
$$k_{obs} = 2k_d K_{et} \qquad (2)$$

where K_{et} is the equilibrium constant of the endergonic electron transfer. Since the free energy change of electron transfer ($\Delta G^0_{et} = -2.3RT \log K_{et}$) is obtained from the E^0_{ox} and E^0_{red} values (Eq. (3)), as in

$$\Delta G^0_{et} = F(E^0_{ox} - E^0_{red}) \qquad (3)$$

where F is the Faraday constant, log k_{obs} is given as a function of E^0_{ox}:

$$\log k_{obs} = \log 2k_d - (F/2.3RT)(E^0_{ox} - E^0_{red}) \qquad (4)$$

Thus, the plot of log k_{obs} versus E^0_{ox} would give a slope of $-(F/2.3RT)$, which corresponds to -17 eV^{-1} at 298 K, provided that the rate constant for deprotonation (k_d) remains constant.[17] The plot of log k_{obs} versus E^0_{ox} is shown in Fig, 3, where the observed slope (-18 eV^{-1}) agrees with that expected from Eq. (3). Moreover, the k_d values derived from the k_{obs} and E^0_{ox} values using Eq. (4) agree well with those determined independently from the first order decay of the radical cations (Table II). Such agreement indicates that the difference in the electron transfer reactivity between the bisphenol and monophenol derivatives results mainly from the difference in their E^0_{ox} values. We ascribe the lower E^0_{ox} values of the bisphenol derivatives to the hydrogen bonding stabilization in the radical cations. The important conclusion here is that intramolecular hydrogen bonding in the radical cation is an essential factor controlling the overall oxidation reactivity in the two-electron oxidation process by decreasing the one-electron oxidation potential.

Hydrogen Transfer Properties of a Series of Bisphenol Derivatives and Monophenol Derivatives

Another important objective of this work was to clarify the effects of the R_1 substituents on the hydrogen transfer properties of the bisphenol derivatives. Thus, the rates of hydrogen transfer reactions of a series of bisphenol derivatives with cumylperoxyl radical to produce phenoxyl radical species were measured using ESR. The cumylperoxyl radical is formed via a photoinduced radical chain process shown in Scheme 4.[11,18–22]
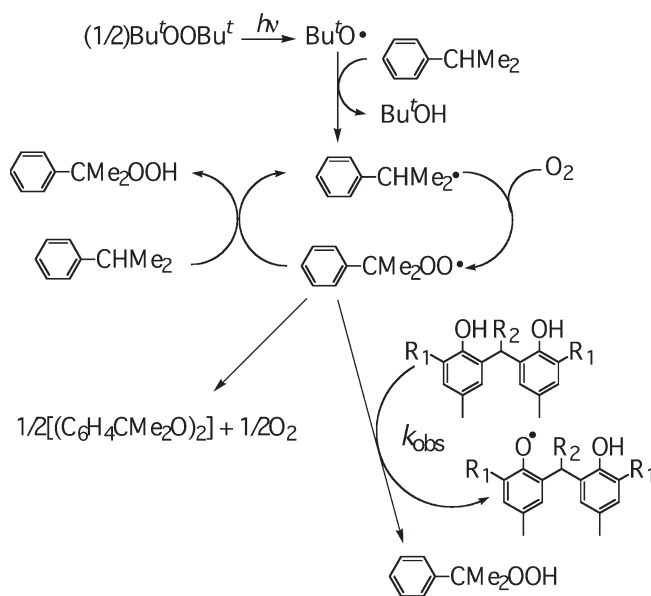
Scheme 4
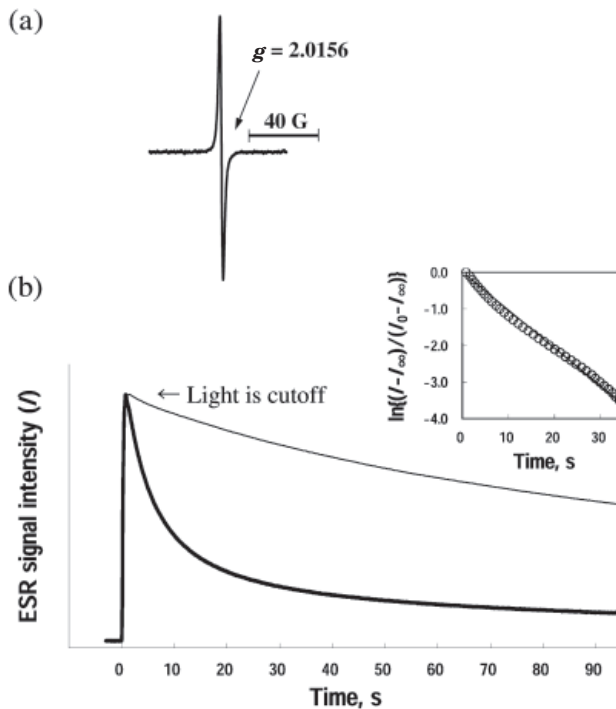
Figure 4. (a) ESR spectra observed in photolysis of an O_2-saturated EtCN solution of di-t-butylperoxide (1.0 M) and cumene (1.0 M) with a 1000 W high-pressure Mercury lamp at 193 K; (b) The decay profiles of the ESR intensity upon light cutoff without (fine line) and with (thick line) a bisphenol derivative ($R_1 = t$–Bu, 1.0×10^{-4} M) in O_2-saturated EtCN at 193 K. Inset shows pseudo-first order plot.

Under photoirradiation of an oxygen saturated propionitrile (EtCN) solution of cumene and di-t-butylperoxide, the O–O bond of the di-t-butylperoxide is cleaved to produce t-bytoxyl radical,[23,24] which abstracts a hydrogen atom from cumene to produce cumyl radical. The cumyl radical is readily trapped by oxygen to produce cumylperoxyl radical. The ESR signal of the cumylperoxyl radical has the typical g value of a peroxyl radical as shown in Fig. 4(a). The cumylperoxyl radical can abstract a hydrogen atom from cumene in the propagation step to yield cumene hydroperoxide, accompanied by regeneration of the cumyl radical (Scheme 4).[25] In the termination step, cumylperoxyl radicals decay via a bimolecular reaction to yield the corresponding peroxide and oxygen (Scheme 4).[25] When illumination is cut off, the decay of the ESR signal intensity corresponding to the cumylperoxyl radical (Fig. 4(a)) obeys second order kinetics owing to bimolecular reaction (Fig. 4(b)). In the presence of a bisphenol derivative, the decay rate of the cumylperoxyl radical after light cutoff becomes much greater than in the absence of a bisphenol derivative. The decay rate in the presence of a bisphenol derivative obeys pseudo-first order kinetics rather than second order kinetics (inset, Fig. 4(b)). Consequently, in the presence of a bisphenol derivative the decay of the ESR signal due to cumylperoxyl radical is ascribed to hydrogen atom transfer from the bisphenol derivative to the cumylperoxyl radical (Scheme 3).

The pseudo-first order rate constant (k) exhibits first order dependence with respect to the concentration of bisphenol or monophenol derivatives (Fig. 5). From the
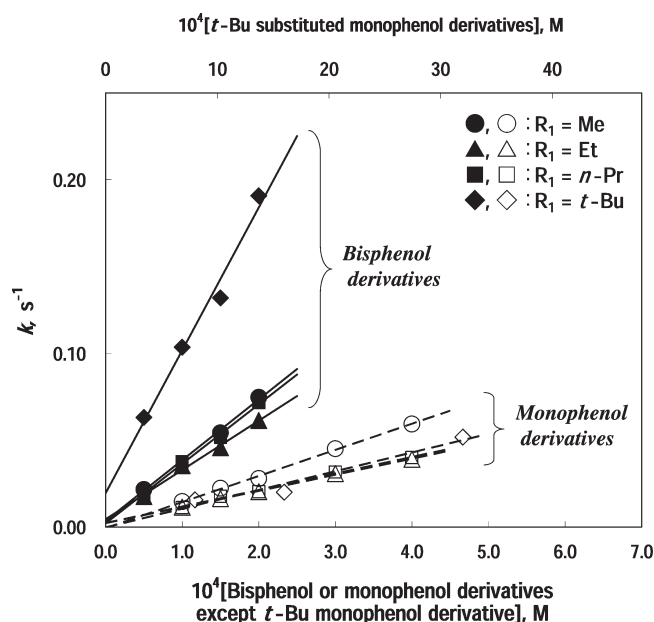
Figure 5. Plots of pseudo-first order rate constant (k) versus concentration of bisphenol or monophenol derivatives in the hydrogen transfer of bisphenol and monophenol derivatives in EtCN containing di-t-butylperoxide (1.0 M) and cumene (1.0 M) at 193 K.

TABLE III. Rate Constants of Deprotonation from Radical Cations (k_d) and Second Order Rate Constants of Hydrogen Transfer Reactions (k_{HT}) of Bisphenol Derivatives

R_1	k_d, [a] s^{-1}	k_{HT}, [b] $M^{-1}s^{-1}$
Me	1.5×10^5	1.8×10^2
Et	1.2×10^5	1.4×10^2
n-Pr	1.1×10^5	1.7×10^2
t-Bu	2.8×10^5	4.1×10^2

[a] Determined from the first order decay of the radical cations using $^1AcrH^{+*}$.
[b] Determined from the hydrogen transfer rate constant using cumylperoxyl radical.

TABLE IV. Relative Ionization and Deprotonation Energies, and HOMO Levels of Bisphenol Derivatives Calculated by the Density Functional Method Using the Gaussian 98 Program

R_1	relative $\Delta\Delta H_f$, kcal mol^{-1} [a]			HOMO, eV
	ionization	deprotonation	total	
Me	0.0	0.0	0.0	−5.36
Et	−1.1	0.7	−0.4	−5.34
n-Pr	−0.8	0.5	−0.2	−5.38
t-Bu	−4.2	−0.4	−4.5	−5.35

[a] Geometry optimizations were carried out by B3LYP/6-31G** basis set.

slopes of these plots we obtain the second order rate constants (k_{HT}) for the hydrogen transfer reaction of the bisphenol derivatives.[26] It was found that t-butyl substituted bisphenol derivatives exhibit the largest rate constant.

The rate constants for the deprotonation of radical cations (k_d) and the second order rate constants for hydrogen transfer (k_{HT}) are summarized in Table III.

The rate constants for the t-butyl substituted bisphenol derivative are more than two times larger than those for the methyl, ethyl, and n-propyl substituted compounds. This indicates that the t-butyl substituent neighboring the hydroxy groups has a significant effect on the intramolecular hydrogen bonding stabilization in both the radical cation and the phenoxyl radical which facilitates the hydrogen transfer step.

Photographic Properties (Sensitometry) of a Series of Bisphenol Derivatives and Monophenol Derivatives

Figure 6(a) shows the characteristic curves of the film samples to which various bisphenol derivatives and monophenol derivatives were added. The development kinetic behavior for methyl-substituted and t-butyl-substituted bisphenol derivatives are shown in Fig. 6(b) and Fig. 6(c), respectively. The development rates of the substituted bisphenol derivatives decrease slightly in order: methyl > ethyl > n-propyl. The t-butyl substituted bisphenol derivative exhibits the highest reactivity of these bisphenol derivatives. As compared to the bisphenol derivatives, the development rates of the monophenol derivatives are significantly lower, regardless of the substituent neighboring the hydroxy group. This may again be ascribed to the hydrogen bonding that stabilizes the oxidized forms of bisphenol derivatives as compared with monophenol derivatives which have no hydrogen bond.

The energies of the neutral compounds, the radical cations, and the phenoxyl radicals were determined from density functional theory (DFT) calculations (see Experimental Section).[27] The relative adiabatic ionization and deprotonation energies, and HOMO levels are listed in Table IV. There is no clear correlation between HOMO levels and calculated ionization energies, whereas both the ionization and deprotonation energies of the t-butyl derivative are the lowest of the bisphenol derivatives in agreement with the highest oxidation reactivity of a t-butyl-substituted bisphenol derivative. This indicates that not only the radical cation but also the deprotonated radical of the t-butyl-substituted bisphenol derivative is most stabilized by the hydrogen bonding. Thus, the low ionization energy of the t-butyl derivative results from the strongest hydrogen bonding, as indicated by the shortest H-bond (see Table II of Ref. 2b).

Conclusion

The main conclusions based on the deprotonation rate constants of radical cations of bisphenol and monophenol derivatives together with the hydrogen transfer rate constants and the developing properties of bisphenol and monophenol derivatives in silver salt photothermographic systems are summarized as follows.

1. Intramolecular hydrogen bonding of radical cations is a main factor in controlling the oxidation of bisphenol derivatives.
2. In our photothermographic system, the t-butyl bisphenol derivative exhibits the highest reactivity of the four bisphenol derivatives.
3. The high reactivity towards oxidation of the t-butyl-substituted bisphenol derivative can be ascribed to the effective intramolecular hydrogen bonding stabilization in the radical cation and also in the phenoxyl radical. ◭

(a)

Legend:
- : R₁ = Me
- : R₁ = Et
- : R₁ = n–Pr
- : R₁ = t–Bu
- : Monophenol derivatives

Y-axis: Optical density
X-axis: log (exposure, mW)

(b)

Legend:
- : 6 sec.
- : 9 sec.
- : 12 sec.
- : 15 sec.

Y-axis: Optical density
X-axis: log (exposure, mW)

(c)

Legend:
- : 6 sec.
- : 9 sec.
- : 12 sec.
- : 15 sec.

Y-axis: Optical density
X-axis: log (exposure, mW)
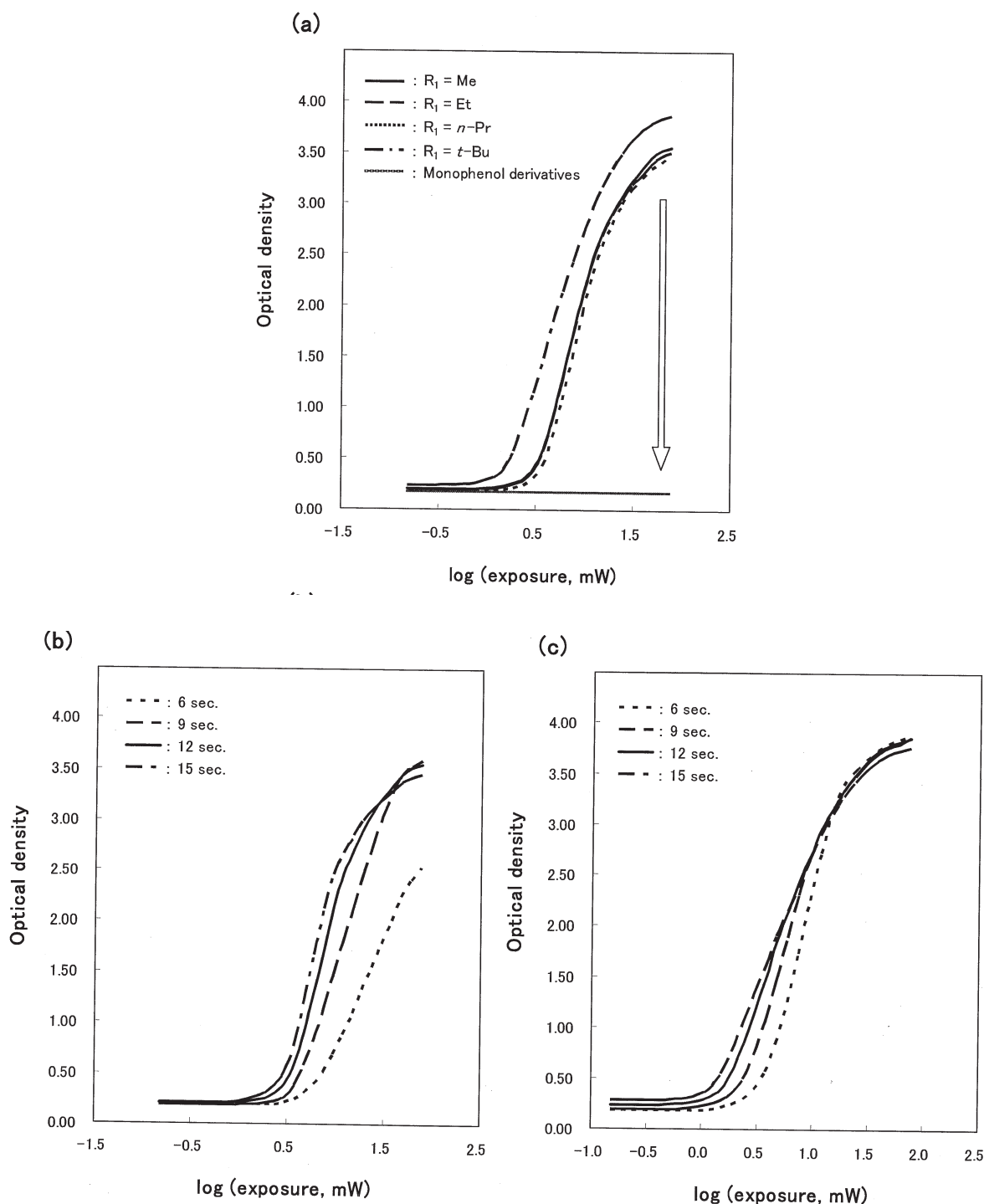
Figure 6. (a) Effects of substituents of bisphenol derivatives and intramolecular hydrogen bonding on photothermographic characteristic curves obtained in the developing process at 399 K. Development kinetics (b) for the methyl-substituted bisphenol derivative and (c) for the t-butyl-substituted bisphenol derivative.

References

1. T. Maekawa, M. Yoshikane, H. Fujimura, and I. Toya, *J. Imaging Sci. Technol.* **45**, 365 (2001).
2. (a) H. Akahori, K. Morita, A. Nishijima, T. Mitsuhashi, K. Ohkubo, and S. Fukuzumi, *J. Soc. Photogr. Sci. Technol. Japan* **66**, 491 (2003); (b) H. Akahori, K. Morita, A. Nishijima, T. Mitsuhashi, K. Ohkubo, and S. Fukuzumi, *J. Imaging Sci. Technol.* **47**, 124 (2003).
3. (a) L. Taimr, H. Pivcova, and J. Pospisil, *Collect. Czech. Chem.*

Commun. **37**, 1912 (1972); (b) L. Taimr and J. Pospisil, *Angew. Makromol. Chem.* **28**, 13 (1973).

4. R. Amorati, M. Lucarini, V. Mugnaini, and G. F. Pedulli, *J. Org. Chem.* **68**, 5198 (2003).
5. (a) L. C. R. Barclay, C. E. Edwards, and M. R. Vinquist, *J. Amer. Chem. Soc.* **121**, 6226 (1999); (b) M. Lucarini, V. Mugnaini, and G. F. Pedulli, *J. Org. Chem.* **67**, 928 (2002).
6. D. D. Perrin, W. L. F. Armarego, and D. R. Perrin, *Purification of Laboratory Chemicals,* 4th ed, (Pergamon Press, Elmsford, New York, 1996).
7. (a) H. E. Ungnade and A. D. McLaren, *J. Amer. Chem. Soc.* **66**, 118 (1944); (b) D. Harper and A. Lambert, GB Patent 1,076,142 (1967).
8. R. M. G. Roberts, D. Ostovic, and M. M. Kreevoy, *Faraday Discuss. Chem. Soc.* **74**, 257 (1982).
9. S. Fukuzumi, S. Koumitsu, K. Hironaka, and T. Tanaka, *J. Amer. Chem. Soc.* **109**, 305 (1987).
10. (a) K. Ohkubo, K. Suga, K. Morikawa, and S. Fukuzumi, *J. Amer. Chem. Soc.* **125**, 12850 (2003); (b) M. Fujita, A. Ishida, S. Takamuku, and S. Fukuzumi, *J. Amer. Chem. Soc.* **118**, 8566 (1996).
11. S. Fukuzumi, K. Shimoosako, T. Suenobu, and Y. Watanabe, *J. Amer. Chem. Soc.* **125**, 9074 (2003).
12. (a) A. D. Becke, *J. Chem. Phys.* **98**, 5648 (1993); (b) C. Lee, W. Yang and R. G. Parr, *Phys. Rev. B* **37**, 785 (1988).
13. W. J. Hehre, L. Radom, P. v. R. Schleyer, and J. A. Pople, *Ab Initio Molecular Orbital Theory*, (Wiley, New York, 1990).
14. K. Morita, US Patent 6,387,608 (2002).
15. (a) D. Rehm and A. Weller, *Ber. Bunsen-Ges. Phys. Chem.* **73**, 834 (1969); (b) D. Rehm and A. Weller, *Isr. J. Chem.* **8**, 259 (1970).
16. Similar transient absorption spectra of phenol radical cation and phenoxyl radical have been reported. T. A. Gadosy, D. Shukla, and L. J. Johnston, *J. Phys. Chem. A* **103**, 8834 (1999).
17. (a) M. S. Ram and J. T. Hupp, *J. Phys. Chem.* **94**, 2378 (1990); (b) S. C. Weatherly, I. V. Yang, and H. H. Thorp, *J. Amer. Chem. Soc.* **123**, 1236 (2001).
18. R. A. Sheldon, in *The Activation of Dioxygen and Homogeneous Catalytic Oxidation*, D. H. R. Barton, A. E. Martell, and D. T. Sawyer, Eds., (Plenum: New York and London, 1993) pp 9–30.
19. G. W. Parshall and S. D. Ittel, *Homogeneous Catalysis*, 2nd ed., (Wiley, New York, 1992) chap. 10.
20. R. Sheldon and J. K. Kochi, *Adv. Catal.* **25**, 72 (1976).
21. A. E. Shilov, *Activation of Saturated Hydrocarbons by Transition Metal Complexes*, (D. Reidel Publishing Co., Dordrecht, The Netherlands, 1984) chap. 4.
22. A. Bottcher, E. R. Birnbaum, M. W. Day, H. B. Gray, M. W. Grinstaff, and J. A. Labinger, *J. Mol. Catal.* **117**, 229 (1997).
23. J. K. Kochi, *Free Radicals in Solution*, Wiley, New York, 1957.
24. (a) J. K. Kochi, P. J. Krusic, and D. R. Eaton, *J. Amer. Chem. Soc.* **91**, 1877 (1969); (b) J. K. Kochi and P. J. Krusic, *J. Amer. Chem. Soc.* **90**, 7155 (1968); (c) J. K. Kochi and P. J. Krusic, *J. Amer. Chem. Soc.* **91**, 3938 (1969); (d) J. K. Kochi and P. J. Krusic, *J. Amer. Chem. Soc.* **91**, 3942 (1969); (e) J. K. Kochi and P. J. Krusic, *J. Amer. Chem. Soc.* **91**, 3944 (1969); (f) J. A. Howard and E. Furimsky, *Can. J. Chem.* **52**, 555 (1974).
25. (a) S. Fukuzumi and Y. Ono, *J Chem. Soc., Perkin Trans.* **2**, 622 (1977); (b) S. Fukuzumi and Y. Ono, *J. Chem. Soc., Perkin Trans.* **2**, 784 (1977).
26. When the hydrogen transfer reactivity per one hydrogen atom of bisphnol derivatives is compared with that of monophenol derivative, the apparent second order rate constants of bisphenol derivatives should be divided by two in consideration of a statistical factor, to obtain k_{HT}.
27. The calculations have been performed at higher levels than those previously reported.[2b]